

# The Fabry-Pérot Interferometer

## Exercises:

1. Mounting the beam expander optics on the He-Ne laser and adjustment.
2. Alignment of the total optical setup (laser, interferometer, monochromator).
3. Observing and interpreting all interference patterns produced by the interferometer when performed in parallel and divergent light.
4. Recording the photomultiplier signal corresponding to the interference pattern from parallel laser light. Determining the finesse.
5. Aligning a mercury lamp as light source instead of the laser. Recording the hyperfine structure spectrum of the green mercury line at 546.07 nm and of the violet one at 404.6 nm. Elaborating these spectra.

## Knowledge required:

Electromagnetic waves, interference, Fraunhofer diffraction, geometrical optics, atomic spectra.

## Bibliography:

The required matter is treated in every textbook of optics, e.g.,

- [1] E. Hecht: Optics
- [2] Optics, by M.V. Klein and T.E. Furtak, Chaps. 3-6;  
Optics, by F.G. Smith and J.H. Thomson, Chaps. 6,9,13,14,15
- [3] R.W. Pohl: Optik und Atomphysik

A profound treatise on the Fabry-Pérot interferometer is given in

- [4] Spectrophysics, by A. Thorne, U. Litzen and S. Johansson (revised edition of the next book)
- [5] Spectrophysics, by A. Thorne, 2nd edition
- [6] Experiments in Modern Physics, by A.C. Melissinos, Chaps. 7

And a special book is

- [7] Fabry-Pérot Interferometer, by G. Hernandez

# Contents

|           |  |           |
|-----------|--|-----------|
| <b>1</b>  | <b>Introduction</b>  | <b>3</b>  |
| <b>2</b>  | <b>Multiple Beam Interference</b>                                    | <b>4</b>  |
| <b>3</b>  | <b>The Fabry-Pérot Interferometer as a Spectrometer</b>              | <b>7</b>  |
| 3.1       | General . . . . .  | 7         |
| 3.2       | Halfwidth and free spectral range of the ideal interferometer . . .  | 8         |
| 3.3       | Restrictions and the real interferometer . . . . .                   | 8         |
| <b>4</b>  | <b>Mount of the Interferometer and its Accessories</b>               | <b>12</b> |
| <b>5</b>  | <b>Adjustment and Alignment</b>                                      | <b>12</b> |
| 5.1       | Mounting and adjustment of the beam expander . . . . .               | 12        |
| 5.2       | Alignment of the laser . . . . .                                     | 15        |
| 5.3       | The deflecting mirror $M_1$ . . . . .                                | 15        |
| 5.4       | Pumping and gas system . . . . .                                     | 16        |
| 5.5       | Alignment of the optical elements after the interferometer . . . . . | 16        |
| 5.6       | Adjusting the interferometer plates . . . . .                        | 18        |
| <b>6</b>  | <b>Setting the Instruments</b>                                       | <b>20</b> |
| 6.1       | The monochromator . . . . .  | 20        |
| 6.2       | The recorder . . . . .   | 21        |
| 6.3       | The photomultiplier . . . . .  | 21        |
| 6.4       | Optimizing the signal and test measurement . . . . .                 | 21        |
| <b>7</b>  | <b>Measurements with the He-Ne Laser</b>                             | <b>22</b> |
| 7.1       | Measuring the Airy function . . . . .                                | 22        |
| 7.2       | Stability of the total experiment . . . . .                          | 22        |
| <b>8</b>  | <b>Measurements of the Hyperfine Structure of Mercury Lines</b>      | <b>22</b> |
| 8.1       | Change of the optical mount . . . . .                                | 22        |
| 8.2       | Measurements with the mercury lamp . . . . .                         | 24        |
| <b>9</b>  | <b>Evaluation and Analysis</b>                                       | <b>24</b> |
| 9.1       | The finesse . . . . .  | 24        |
| 9.2       | The stability . . . . .  | 25        |
| 9.3       | The refractive index of argon . . . . .                              | 25        |
| 9.4       | Analysis of the hyperfine structure spectra . . . . .                | 25        |
| <b>10</b> | <b>Annex</b>   | <b>29</b> |

# 1 Introduction

An interferometer is a device to make light beams interfere. A light beam is the totality of light rays which enter an optical element (lens, mirror, etc.), the area of which is limited by a diaphragm. The diaphragm may be realized by the edge of the element itself. According to the difference of phase between the beams, the interference pattern will have any degree of brightness. When the phase difference locally changes over the cross section of a beam, the interference pattern is structured and interference fringes can be observed (stripes, rings, and other curves).

The smallest number of beams to achieve interference is two. The Michelson interferometer belongs to the class of two beam interferometers. The light beams coming from the grooves of a diffraction grating interact to a multiple beam interference. Here, the number of interfering beams is still limited, though very large,  $10^3 \dots 10^5$ . In a Fabry-Pérot interferometer (Fig. 1), which is another device to present multiple beam interference, the number of interfering beams is unlimited. It consists of two very plane glass flats in parallel mounting, in which the inner faces have a reflection coefficient close to one. The mirrors of a He-Ne laser cavity, which is indeed a Fabry-Pérot interferometer, reflect at more than 99%, while in our instrument the coefficient is at 0.94.

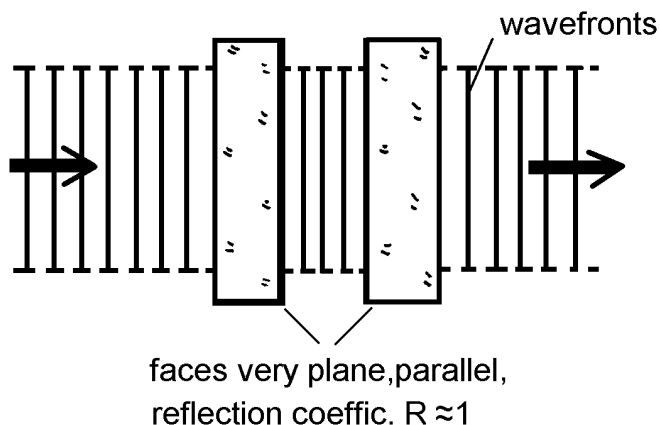


Figure 1: The Fabry-Pérot interferometer

Due to the highly reflecting plane surfaces facing each other in parallel mounting, an infinite number of parallel beams comes out from the right plate (Fig. 1). They are all superimposed, eventually with a slight lateral displacement in case of non-normal incidence of the parallel light on the left plate. The beams distinguish from each other by the number of runs between the pair of reflecting planes of the glass plates. When infinitely many waves are superimposed, of course with decreasing amplitude, constructive interference will be extremely sharp. Therefore, to observe such an interference pattern, the light must be extremely monochro-

matic and the reflecting faces extremely plane.

This experiment deals with multiple beam interference in a Fabry-Pérot interferometer.

## 2 Multiple Beam Interference

Slightly divergent monochromatic light enters the two glass plates in Fig. 2. Their four surfaces are very plane, the inner ones are parallel to each other and highly reflecting. To guide reflections from the outer faces away, the glass plates are wedged at  $0.5^\circ$ . The interference of light from the inner faces is calculated by adding up the amplitudes of all beams leaving the right plate. For the mathematical treatment we can interpret the divergent beam at the entrance of the plates as a superposition of an infinite number of parallel beams with individual angles of incidence,  $\varphi$ , and amplitudes  $E_0(\varphi)$ . The transmission and reflection coefficients of the reflecting films on the plates are  $T$  and  $R$ , respectively, both related to the intensity. There is a phase shift  $\alpha_T$  after passage through a film in the order glass – film – medium between the plates. With each reflection at a film surface, a phase shift of  $-\alpha_R$  happens when the wave enters the film from the side of that medium. In the entity of beams leaving the interferometer at its right side, two successive beams differ by the bold geometrical path  $s$  in Fig. 2, we will call the corresponding optical path difference  $\delta$  with  $\delta = ns$ . A few pages ahead,  $\delta$  will be calculated;  $\delta$  is a function of the angle of incidence,  $\varphi$ . At the exit of the second glass plate, the beams have the following amplitudes,  $\sigma = 1/\lambda$  (inverse vacuum wavelength):

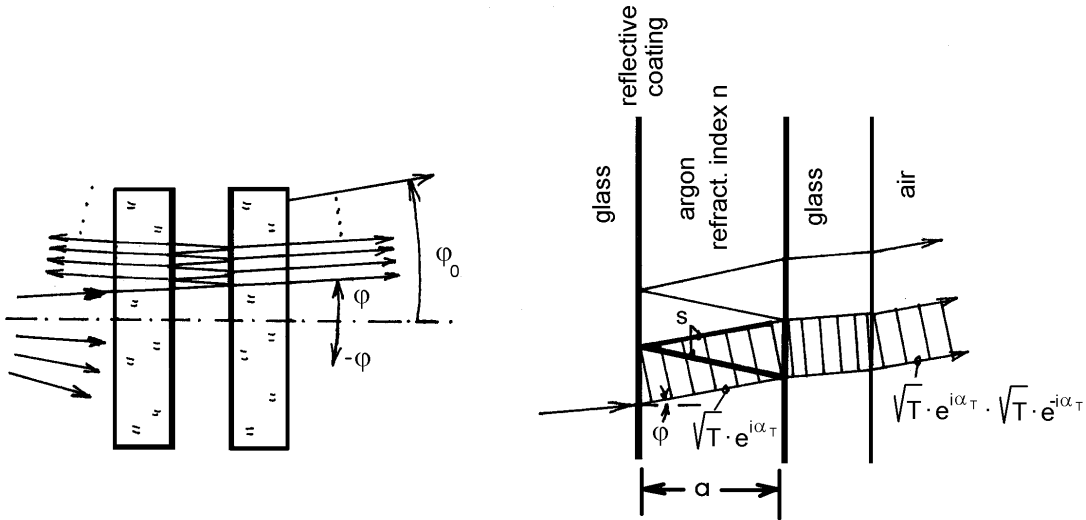


Figure 2: Multiple beam interference and mutual optical path difference

1st beam:

$$E_1 = E_0(\varphi)\sqrt{T}e^{i\alpha_T} \cdot \sqrt{T}e^{-i\alpha_T}e^{i2\pi\sigma n\frac{a}{\cos\varphi}} = T E_0(\varphi)e^{i2\pi\sigma n\frac{a}{\cos\varphi}} ;$$

2nd beam:

$$E_2 = E_1\sqrt{R}e^{-i\alpha_R}e^{-i2\pi\sigma\delta}\sqrt{R}e^{-i\alpha_R} = TE_0(\varphi)e^{i2\pi\sigma n\frac{a}{\cos\varphi}} Re^{-i(2\alpha_R+2\pi\sigma\delta)} ;$$

3rd beam:

$$\begin{aligned} E_3 &= E_2Re^{-i(2\alpha_R+2\pi\sigma\delta)} = TE_0(\varphi)e^{i2\pi\sigma n\frac{a}{\cos\varphi}} \left[Re^{-i(2\alpha_R+2\pi\sigma\delta)}\right]^2 , \\ &\vdots \end{aligned} \quad (1)$$

The sum of these amplitudes is the geometrical series

$$\begin{aligned} \frac{E(\varphi)}{E_0(\varphi)} &= T e^{i2\pi\sigma n\frac{a}{\cos\varphi}} \left( 1 + Re^{-i(2\alpha_R+2\pi\sigma\delta)} + \left[Re^{-i(2\alpha_R+2\pi\sigma\delta)}\right]^2 + \dots \right) \\ &= \frac{T e^{i2\pi\sigma n\frac{a}{\cos\varphi}}}{1 - Re^{-i\phi}} , \end{aligned} \quad (2)$$

$$\text{where } \phi = 2\alpha_R + 2\pi\sigma\delta .$$

To obtain this result, take into account that  $R < 1$ ,  $n \rightarrow \infty$ , and therefore

$$\left[Re^{-i(2\alpha_R+2\pi\sigma\delta)}\right]^n \rightarrow 0 .$$

The observable signal in optical waves is the intensity. It will come out that the intensity depends on  $\sigma$ ,  $n$ ,  $a$ ,  $\varphi$ , which are all implied in  $\phi$ , so we write  $I(\phi)$  for the intensity. It is

$$\begin{aligned} \frac{I(\phi)}{I_0(\varphi)} &= \frac{E(\phi)}{E_0(\varphi)} \cdot \left( \frac{E(\phi)}{E_0(\varphi)} \right)^* \\ &= \frac{T^2}{|1 - R \cos \phi + iR \sin \phi|^2} = \frac{T^2}{(1 - R)^2} \frac{1}{1 + M \sin^2 \frac{\phi}{2}} \\ &\text{with } M = \frac{4R}{(1 - R)^2} . \end{aligned} \quad (3)$$

Equation (3) is known as the Airy distribution. Preceding a discussion,  $\delta$  shall be calculated. Thus, we can see which parameters influence  $\phi$  in the Airy distribution.

The geometrical path difference  $s$  (two bold paths in Fig. 2) between two successive beams is

$$s = \frac{a}{\cos \varphi} + \frac{a}{\cos \varphi} \cos 2\varphi = 2a \cos \varphi$$

and from that

$$\delta = ns = 2na \cos \varphi \quad (4)$$

and finally

$$\frac{\phi}{2} = \alpha_R + 2\pi n\sigma a \cos \varphi . \quad (5)$$

Figure 3 presents the Airy distribution as a function of  $\phi$ . As  $\phi$  depends linearly on  $n$ ,  $\sigma$ ,  $a$ , and  $\cos \varphi$ , we may imagine that the abscissa is scaled with anyone of these four parameters. The phase shift  $\alpha_R$  may be set to zero, because we shall be interested only in the difference of  $\phi$  values. The closer the reflection coefficient  $R$  is to one, the larger is  $M$  and the sharper are the maxima of the Airy distribution. For parallel light at any incidence  $\varphi$  on the reflective films, there is a standing wave in the medium between the glass plates, whenever  $I(\phi/2)$  is at one of its maximum values (Fig. 3). Indeed, it follows from Eq. (5) for these points

$$\frac{\phi}{2} = m \cdot \pi = 2\pi n\sigma a \cos \varphi \quad \text{or} \quad na \cos \varphi = m \frac{\lambda}{2}, \quad (6)$$

where  $m$  is an integral number called order of interference. Equation (6) means that the optical path of a slightly inclined beam between the mirrors is a multiple of half the wavelength. So there is resonance in the peaks of the Airy distribution. Therefore, the Fabry-Pérot interferometer is also called optical resonator or cavity. The laser is an immediate application of this feature.

The factor  $\left(\frac{T}{1-R}\right)^2$  in Eq. (3) can be replaced by  $\left(\frac{T}{T+A}\right)^2$  because of

$$R + T + A = 1 ,$$

where  $A$  is the absorption of the film. The factor becomes unity for materials without absorption. Such materials are dielectric. Metallic films absorb more or less; in visible light silver is a good choice.

The extrema of the Airy function are obviously

$$\begin{aligned} I_{\max} &= \left(\frac{T}{1-R}\right)^2 I_0 = \left(\frac{1-R-A}{1-R}\right)^2 I_0 , \\ I_{\min} &= \left(\frac{T}{1-R}\right)^2 \frac{1}{1 + \frac{4R}{(1-R)^2}} I_0 = \left(\frac{T}{1+R}\right)^2 I_0 = \left(\frac{1-R-A}{1+R}\right)^2 I_0 . \end{aligned} \quad (7)$$

Divergent light (or convergent beyond its focus) after passing a pair of Fabry-Pérot plates has a beautiful annulus system as an interference pattern (Fig. 4). These extremely sharp fringes are named Haidinger rings or fringes of equal inclination. On such a fringe the angle  $\varphi$ , which a beam tends with the optical axis (Fig. 2), is constant. Haidinger rings are localized at infinity, therefore when looking into the interferometer, the eye must be completely detented to see them.

From the sharpness of interference fringes one can immediately see whether they are a two beam or a multiple beam phenomenon. Two beam interference

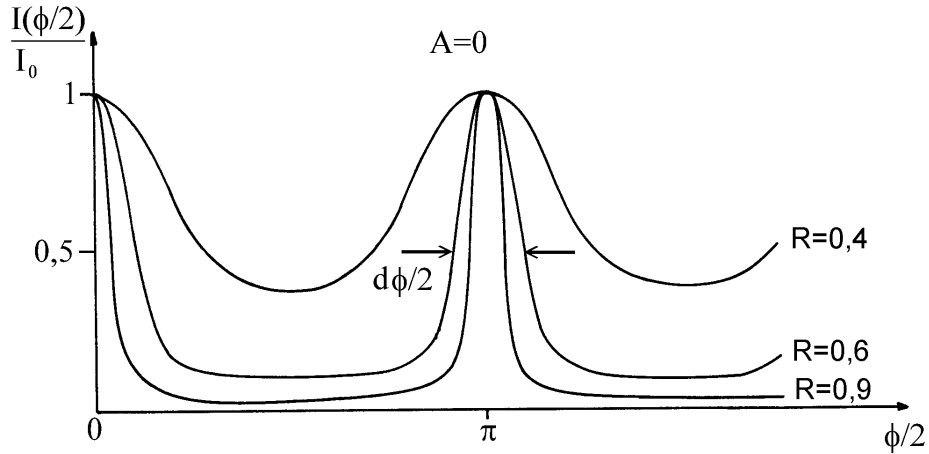


Figure 3: Airy function for different reflection coefficients  $R$

produces cosine fringes, whereas from multiple interference extremely sharp patterns are obtained, they look as if they were grooved with a needle. In order to have a measure of the sharpness the term finesse has been introduced. It is the ratio between the distance of two neighbour peaks (Fig. 3) and their halfwidth. The finesse of a Fabry-Pérot interferometer can be pushed up to  $> 200$ . But to achieve such a result the plates have to be extremely plane and the coating must have a reflection coefficient of nearly one. The alignment must be perfect and the light must be parallel.

### 3 The Fabry-Pérot Interferometer as a Spectrometer

#### 3.1 General

When the light entering the interferometer is not monochromatic there will be an Airy function for each wave number  $\sigma$  contained in the spectrum of the light source. For unambiguity the region of the spectral emission of the source,  $\sigma_{\max} - \sigma_{\min}$ , must fit into the gap between two neighbour peaks of the Airy function. As the principal application of the Fabry-Pérot interferometer is spectroscopy of hyperfine structure, the required spectral resolution  $d\sigma$  is some  $10^{-2} \text{ cm}^{-1}$  corresponding to  $d\lambda \approx 10^{-3} \text{ nm}$ . Therefore the relations between the instrument parameters and the resolution shall be treated.

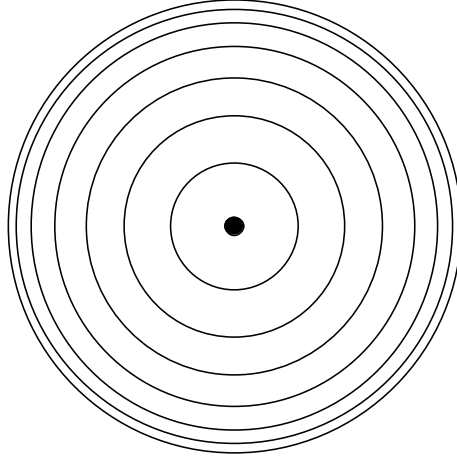


Figure 4: Fringes of equal inclination, also called Haidinger fringes

### 3.2 Halfwidth and free spectral range of the ideal interferometer

The halfwidth of the Airy function,  $d\frac{\phi}{2}$ , is obtained from

$$\frac{1}{2} = \frac{1}{1 + M \sin^2\left(\frac{1}{2} d\frac{\phi}{2}\right)}, \quad \text{with } M = \frac{4R}{(1-R)^2}$$

as

$$d\frac{\phi}{2} \approx \frac{2}{\sqrt{M}} = \frac{1-R}{\sqrt{R}} = 2\pi n a \cos \varphi d\sigma. \quad (8)$$

The free spectral range, i.e.,  $\Delta\sigma = \sigma_{\max} - \sigma_{\min}$ , fitting into the gap between two successive maxima of the Airy function (Fig. 5) is found from

$$\Delta\frac{\phi}{2} = 2\pi n a \cos \varphi \Delta\sigma = \pi \quad \text{as} \quad \Delta\sigma = \frac{1}{2na \cos \varphi}. \quad (9)$$

### 3.3 Restrictions and the real interferometer

The conditions leading to (8) and (9) have been that the following parameters are constant over the cross section of the interferometer plates, that is over the field of view:

- distance between the reflecting faces,  $a$ ,
- inclination  $\varphi$  of the parallel light; remember that within the divergent beam of light (Fig. 2) we ignored all directions but  $\varphi$ ,
- reflection coefficient  $R$  and index of refraction  $n$ .

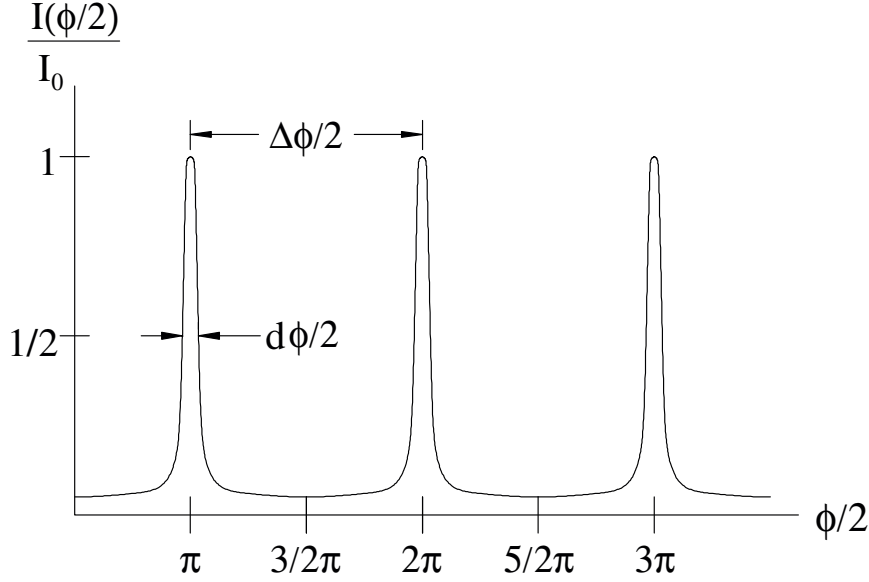


Figure 5: Halfwidth and free spectral range

The parameters  $R$  and  $n$  are obviously constant. This is guaranteed by the process of evaporating thin films and, as for  $n$ , by the medium between the plates, which is a gas.

But neither  $a$  nor  $\varphi$  are constant. Even if the reflecting faces are well aligned and therefore parallel they are not perfectly flat. Typical deviations of their topography from a plane are  $\lambda/10$  to  $\lambda/200$ , where  $\lambda$  is about 500 nm. Therefore  $a$  is not constant, and each zone on the interferometer plates has its own value of  $\phi/2$  to come to a maximum of the Airy function. The result is a broadening of the peaks.

By the same argument there is an additional broadening when the light is divergent instead of parallel. Notice that a divergent beam can be thought to be composed of parallel beams of individual inclinations  $\varphi$ .

So finally there are three effects restricting the spectral resolution  $d\sigma$ , namely

- the limited reflection ( $R < 1$ ),
- the finite flatness of the reflective faces,
- the residual divergence of the light entering the interferometer.

The halfwidth  $d\frac{\phi}{2}$  calculated from (8) must be completed. As the three effects are mutually independent we have to sum up the squares of their corresponding  $d\frac{\phi}{2}$  to find the total width of the peaks of the Airy function. From (5) we get the width of the peaks of the Airy curve,  $\left(d\frac{\phi}{2}\right)_a$ , when the flatness of the mirrors is limited and the rest of the instrument is perfect ( $R = 1$ ,  $\varphi = \text{const.}$ , etc.). It is

$$\left(d\frac{\phi}{2}\right)_a = 2\pi n\sigma \cos \varphi da = \pi \frac{2da}{\lambda}, \quad (10)$$

because we can set  $n \approx 1$  and  $\varphi \approx 0$ . The precision of optical surfaces is always given in fractions or multiples of the wavelength. Usually the reference wavelength is 500 nm. When the deviation from flatness,  $da$ , is the  $\mu$ -th fraction of  $\lambda$ , then we obtain

$$\left(d\frac{\phi}{2}\right)_a = \pi \frac{2}{\mu}. \quad (11)$$

In the actual interferometer the mirrors have a quality of  $\lambda/50$ . So it is

$$\left(d\frac{\phi}{2}\right)_a = \frac{\pi}{25}. \quad (12)$$

Again from (5) we obtain the broadening of the peaks  $\left(d\frac{\phi}{2}\right)_\varphi$  when the light is divergent, actually

$$\left(d\frac{\phi}{2}\right)_\varphi = 2\pi n a \sigma d(\cos \varphi), \quad (13)$$

where  $-\varphi_{\max} < \varphi < +\varphi_{\max}$  and  $2\varphi_{\max} = \vartheta = \frac{d}{f}$ .  
This time  $R = 1$  and  $a = \text{const}$  is supposed.

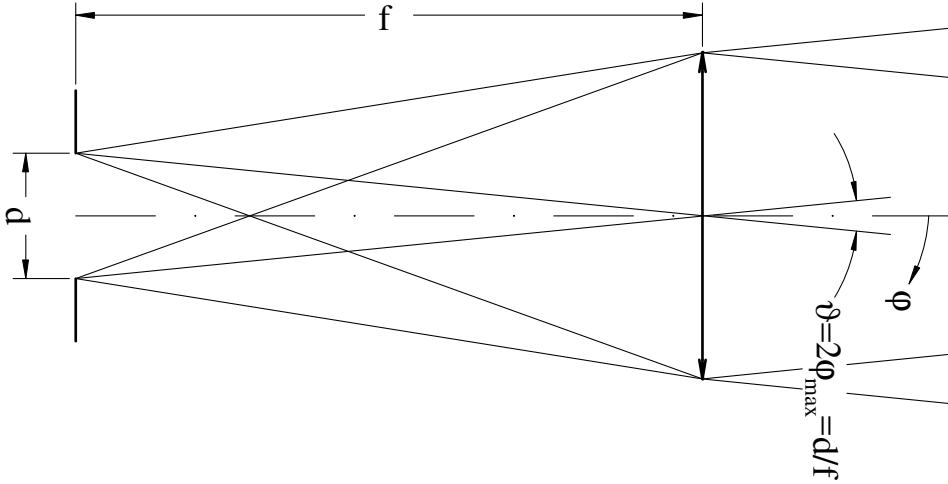


Figure 6: Divergence and diameter of diaphragm

Figure 6 shows how the divergence is defined by the diameter  $d$  of the diaphragm conjugated to the light source and the focal distance  $f$  of the collimator lens. The diaphragm serves as a spatial filter. The variation of  $\cos \varphi$  over the field of view,  $d(\cos \varphi)$ , is

$$d(\cos \varphi) = \cos \varphi_{\max} - \cos 0 \approx -\frac{\varphi_{\max}^2}{2} = -\frac{\vartheta^2}{8} = -\frac{d^2}{8f^2},$$

and from the preceding equation we obtain

$$\left(d\frac{\phi}{2}\right)_{\varphi} = 2\pi na\sigma \frac{\vartheta^2}{8} = \pi na\sigma \frac{d^2}{4f^2}. \quad (14)$$

Calculating the three components of the total  $d\frac{\phi}{2}$ , equipartition of the light intensity over  $a$  and  $\vartheta$  was assumed. This is not necessarily correct. But because the real partitions are unknown we stay with this simple assumption.

With each of the three  $d\frac{\phi}{2}$  just calculated, a finesse of its own is defined, actually

$$F_R = \frac{\pi}{\left(d\frac{\phi}{2}\right)_R} = \frac{\pi\sqrt{R}}{1-R}, \quad F_a = \frac{\pi}{\left(d\frac{\phi}{2}\right)_a} = \frac{\mu}{2} = 25, \quad F_{\varphi} = \frac{\pi}{\left(d\frac{\phi}{2}\right)_{\varphi}} = \frac{4}{a\sigma\vartheta^2} = \frac{4f^2}{a\sigma d^2}. \quad (15)$$

The index  $R$  signifies the obstruction due to the finite reflection coefficient  $R$ . The total finesse,  $F$ , measured in the experiment is got from

$$\left(d\frac{\phi}{2}\right)^2 = \sum \left(d\frac{\phi}{2}\right)_{\text{individual}}^2 = \sum \frac{\pi^2}{F_{\text{individual}}^2} = \frac{\pi^2}{F^2} \quad (16)$$

or

$$\frac{1}{F^2} = \frac{1}{F_R^2} + \frac{1}{F_a^2} + \frac{1}{F_{\varphi}^2}. \quad (17)$$

From (16), (8), (11), and (14) the total width of the Airy function is obtained, it is

$$\left(d\frac{\phi}{2}\right)^2 = \left(\frac{1-R}{\sqrt{R}}\right)^2 + \frac{4\pi^2}{\mu^2} + \frac{\pi^2 n^2 a^2 \sigma^2 d^4}{16 f^4}. \quad (18)$$

The total width  $d\frac{\phi}{2}$  limits the spectral resolution,  $d\sigma$ , according to (8):

$$d\sigma = \frac{d\frac{\phi}{2}}{2\pi na \cos \varphi} \approx \frac{d\frac{\phi}{2}}{2\pi a}; \quad (19)$$

$d\frac{\phi}{2}$  must be taken from (18).

Unlike a monochromator, our F.P. interferometer scans the refractive index  $n$  and not  $\sigma$ , which is performed by means of the gas pressure. The peaks generated by a monochromatic spectral line have a width

$$dn = \frac{d\frac{\phi}{2}}{2\pi a\sigma \cos \varphi} \approx \frac{d\frac{\phi}{2}}{2\pi a\sigma} \quad (20)$$

or, because  $n - 1 \sim p$ ,

$$dp = \frac{\text{const} \cdot d\frac{\phi}{2}}{2\pi a\sigma \cos \varphi} \approx \frac{\text{const} \cdot d\frac{\phi}{2}}{2\pi a\sigma}, \quad (21)$$

again,  $d\frac{\phi}{2}$  to be taken from (18).

An important statement is that at a given pair of F.P. plates (i.e., at fixed flatness and reflection coefficient) and at a fixed entrance diaphragm ( $d$  defined by the required intensity of light), the spectral resolution can be pushed extremely high by increasing the thickness of the etalon, i.e.,  $a$ . But this is on the dispense of free spectral range, see (9).

## 4 Mount of the Interferometer and its Accessories

The total mount is shown in Fig. 7. The interferometer is mounted in a little recipient which can be evacuated and slowly refilled with argon to scan the phase  $\frac{\phi}{2}$  by increasing the refractive index  $n$  from 1 to 1.00026. During the scanning the transmitted light is recorded by a photomultiplier fixed behind the exit slit of grating double monochromator. The monochromator (Fig. 8) keeps all spectral lines out apart from the line in question, for example the green mercury line at 546.07 nm. Two light sources are on disposition, actually a He–Ne laser and a mercury lamp of low pressure.

The laser emits a spectral line which is by far too narrow to be resolved by the interferometer. The recorded response to such a line is called instrument function, because the spectral light distribution at its entrance is considered as a delta function. Therefore the He–Ne laser is a light source to reveal the finesse and the instrument function of this F.P. interferometer.

The mercury lamp serves as a source to perform a hyperfine structure spectrum. Good lines for this demonstrations are at 547.07 nm and 404.6 nm, they are bright and narrow. To avoid Doppler and pressure broadening the discharge is kept at room temperature and the corresponding saturation pressure.

The laser is equipped with a beam expander and a spatial filter in order to form a beam with very plane wavefronts. The beam expander must be mounted and adjusted on a separate linear bench.

## 5 Adjustment and Alignment

### 5.1 Mounting and adjustment of the beam expander

Put the laser on a separate linear bench on the table instead of that one below it, handling will be easier. Direct the laser beam into the center of the system of concentric circles drawn on a white cardboard, which is part of the equipment. Screw the mount of the objective  $L_0$  on the laser housing and tighten by means of the disk on the thread. Adjust  $L_0$  until the divergent light beam beyond the focus is centered on the circles on the cardboard.

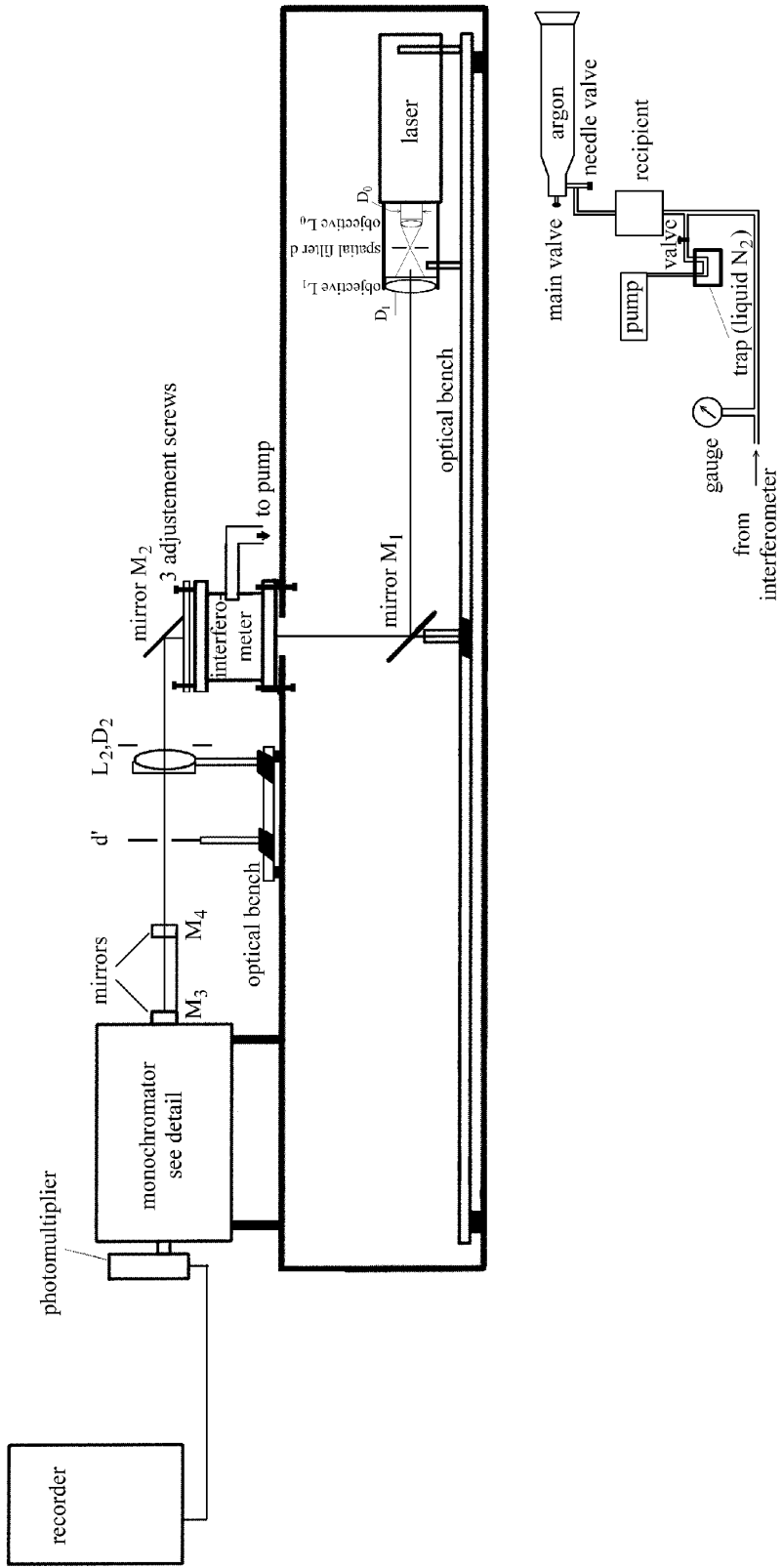


Figure 7: The complete mount

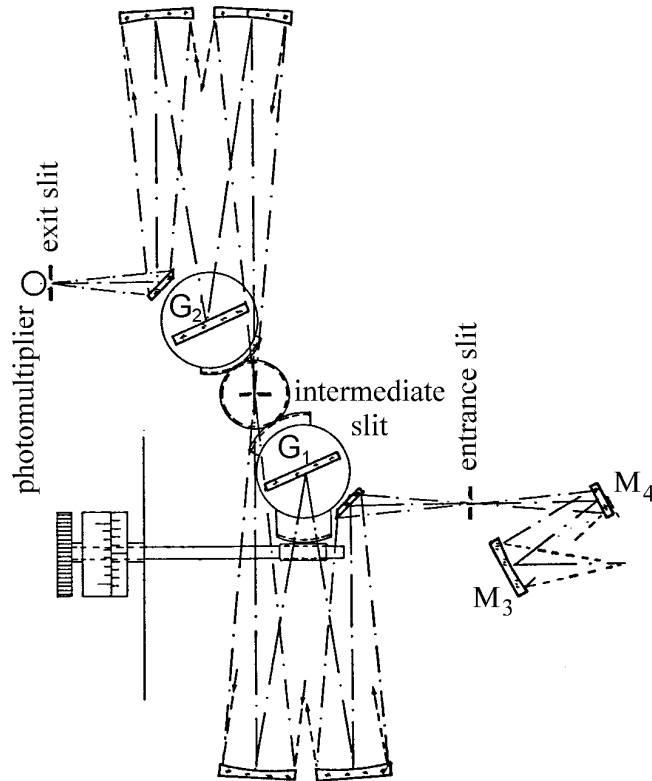


Figure 8: The monochromator

Next, mount that part of the beam expander which contains the spatial filter. The usual situation now is, that the light completely fails the pinhole, the diameter of which being only  $30\ \mu\text{m}$ . Switch off the lights and look from the side on the edge of the pinhole. It shimmers faintly reddish. With the two adjustment screws you can make the shimmer brighter till finally pinhole and focus spot coincide. Actually there are many focus points, namely one for each discrete direction of light within the beam emitted by the laser. If your adjustment is correct, the big red spot on a cardboard or on the white wall of the laboratory has a strict rotational symmetry. Generally, there will be a diffraction pattern on that spot on the wall. Even if only the Airy disk and a part of the first dark ring can be seen, it indicates that the edge of the pinhole cuts into the light beam. Adjust the pinhole in axial sense till the light distribution over the spot is uniform. There is a special little wrench which fits into the mount of the pinhole; turn this mount only by a few degrees to find the correct longitudinal position of the pinhole.

Screw the tube with the objective  $L_1$  on the spatial filter to complete the beam expander.  $L_1$  must be displaced forth or back until its focal point coincides with the pinhole of the spatial filter and the light leaving the expander is parallel. This adjustment must be performed observing interferences fringes generated by a shearing plate.

The objective  $L_1$  is set correctly and the light is parallel, when the spacing of the interference fringes is at maximum. For details see the annex to these instructions.

After these procedures the beam expander is completely adjusted. However, now and then you must check if the spatial filter is still in the correct lateral position.

## 5.2 Alignment of the laser

Put the laser on the bench below the table, the cap with the little hole on the exit objective of the expander. From now the thin beam shaped by the little hole in the cap will be called ray, when the cap is off we call it beam. Define a mark on the cylindrical body of the laser (e.g., label of production) and keep it always in the same azimuthal position. This is necessary because the optical axis of the beam and the mechanical axis of the cylinder are mutually inclined.

Align the laser ray precisely parallel to the bench at the height of the center of the mirror which is to deflect the laser light into the interferometer. For the alignment use the special rod clamped in a sliding mount.

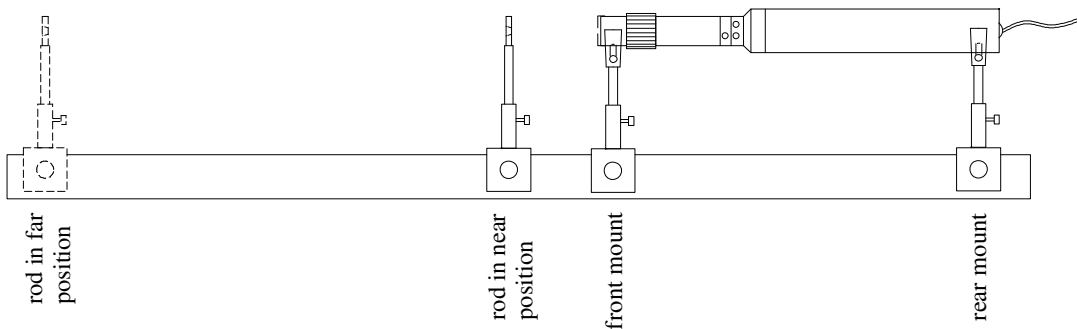


Figure 9: Aligning the laser on the optical bench

The rod has a pinhole drilled precisely across its axis. Bring the rod in the near position to adjust the front mount of the laser, then slide it into the far position to adjust the rear mount (Fig. 9). Repeat this procedure until the red annulus encircling the pinhole in the rod remains centered in the near and far position.

## 5.3 The deflecting mirror $M_1$

Place the sliding mount with the deflecting mirror on the bench at the intersection with the axis of the interferometer. Set the inclination of the mirror so that the brightest among all beams reflected from the interferometer re-enters the hole in the cap on the laser. Find a position of the sliding mount on the bench to center the laser ray on the exit window of the interferometer.

For all alignments after the interferometer the transmitted light shall have maximum brightness. Adjusting the inclination of the deflecting mirror was favoured by maximum intensity of the reflected light. Transmitted and reflected light complete to unity if there is no absorption in the thin films on the F.P. plates. From the shape of the Airy curve it follows that there is strong reflection at nearly every pressure in the interferometer but poor transmission. Therefore, for all further alignments the pressure must be set to obtain maximum transmission. A short instruction is given how to operate the gas inlet and pumping equipment. Respect it seriously because any mistake impairs the quality of all optical elements inside the interferometer.

## 5.4 Pumping and gas system

A sketch of the system is comprised in Fig. 7. The pump is filled with oil. To protect the optical surfaces from pollution the access to the interferometer etc. is only through the trap cooled with liquid nitrogen. When the pump is in standby mode, atmospheric air slowly leaks in. Therefore, whenever you open the valve between pump and recipient – in the sketch simply called valve – be sure that

- the pump is running
- and the trap is filled with liquid nitrogen.

Close the valve before you switch off the pump.

All types of vapour are frozen in the trap, in particular  $\text{H}_2\text{O}$ , wherefore the pressure in the interferometer is very constant even when pumping or refilling is stopped at intermediate values between vacuum and atmospheric pressure. The final pressure attained after a few minutes pumping is some  $10^{-2}$  mbar, although the gauge then indicates about 5 mbar.

When the system is evacuated close valve and pump as described and let argon in. First open the main valve on the big storage bottle while the needle valve is still closed. There is no reduction valve, which means that the 200 bar in the bottle act on the needle valve. It is harmless unless you do stupid things. Slowly open the needle valve while watching the gauge, the needle valve has a backlash of about half a turn. When you close it do not tighten, the thread is very fine.

## 5.5 Alignment of the optical elements after the interferometer

### a) The principle.

The mercury lamp used later in this experiment emits more lines than the green one at 540.67 nm. These lines must be kept away from the photomultiplier to avoid ambiguity; therefore the monochromator is part of the optical configuration.

The parallel beam coming out of the interferometer must be focalized on the entrance slit of the monochromator (Fig. 8) and enter it in a given direction in order to cover the diffraction grating completely. Fixed with the monochromator there is a concave and a plane mirror ( $M_3$  and  $M_4$ , resp.) which form an image of a light source on the entrance slit with a magnification of unity.  $M_3$  and  $M_4$  are adjusted that way that the grating  $G_1$  is fully illuminated, when an image of the lamp covers the entrance slit. To keep this adjustment the positions of  $M_3$  and  $M_4$  must not be changed.  $M_3$  is conjugated to  $G_1$  and  $G_2$  and must therefore be symmetrically and fully illuminated. An image of the source must symmetrically cover the entrance slit. To achieve the latter, the objective  $L_2$  must form an intermediate image of the spatial filter (pinhole, see beam expander) at the appropriate distance in front of the concave mirror  $M_3$ .

**b) Alignment of mirror  $M_2$**

Mirror  $M_2$  is mounted on a plate which has three screws for alignment. They allow to align the direction of the laser ray in horizontal and vertical sense. However, the adjustments are not mutually independent. Therefore, think about the axis around which the ray will rotate before you turn one of the screws. In addition, the vertex of the angle of deflection performed by  $M_2$  can be lifted or lowered when turning all screws. The position of the monochromator must not be changed. For the alignment the following information is helpful: The ray is parallel to the plane of the wooden table when it enters the monochromator correctly.

Put the short bench with the objective  $L_2$  aside and align the ray parallel to the plane of the table, use the special rod. Once the ray is parallel it is easy to make it hit the center of the concave mirror  $M_3$  and the center of the entrance slit.

**c) Alignment of the short bench on the table**

Align the short bench by means of the special rod so that bench and laser ray are parallel. The gap between the bench and the interferometer shall be about 10 mm.

**d) Aligning the objective  $L_2$**

$L_2$  must be positioned in such a manner that the laser ray is not deflected and that there is a sharp image of the pinhole inside the beam expander on the entrance slit of the monochromator. The objective is fixed in an eccentric mount. Rotating and lifting the mount,  $L_2$  can be aligned. It is useful first to align by means of the laser ray, then pull off the cap of the beam expander, correct the alignment, and focus precisely. The correct position of  $L_2$  is very close to the interferometer. You will remark that there is a lot of images in the focal plane of the objective and so in the plane of the slit. Decide for the brightest spot, it is the correct one. Think about the origin of the others, their location and their assumed behaviour during scanning. We call these images aberrated and their generative beams aberrated beams. They must not be confused with lens

aberrations. The concave mirror  $M_3$  is inclined with respect to the direction of the incident light, so the image on the entrance slit is astigmatic. This means that  $M_3$  forms two separated images of the pinhole on the slit, one behind the other, i.e., a short vertical line, called tangential or meridional image, and another one, which is horizontal and its description is sagittal image. Of course, the tangential image guarantees the best separation from the aberrated spots.

#### e) The pinhole disk

The pinhole disk must be placed on the intermediate image of the pinhole in the beam expander generated by the lens  $L_2$ . The little hole in the disk is an additional spatial filter. When you look at the mount of the disk you see immediately how it can be aligned.

## 5.6 Adjusting the interferometer plates

This adjustment shall be done last in order to spend only little time until the measurement starts. There will be no noticeable change of direction of the beam coming out of the interferometer, because the correction to be done now is tiny.

By means of a steel ring, called etalon, the plates are separated at a distance  $a = 5.231$  mm. The ring is polished and has very parallel faces, but the parallelism is still not good enough for the experiment. In Fig. 10 the interferometer is drawn in a section containing the optical axis, and the procedure to improve the parallelism can be understood. The etalon (4) is milled such a way that the interferometer plates lie on three points separated by  $120^\circ$  of rotation. At these points three rectangular levers (each consisting of parts 1a, b, and pivot  $G$ ) gently act on the plates and deform them by a fraction of a wavelength. Thus the parallelism can be improved. The levers are preadjusted by means of a spring pressed by a screw (7), which can only be done when the interferometer is opened. At the end of each lever there is a magnet  $M$ , which is more or less attracted from outside depending how close the magnet  $M'$  is approached to the wall of the instrument.

So far the mechanism to modify the space between the plates. To judge how parallel they are interference fringes must be generated, actually fringes of equal inclination, also called Haidinger fringes (Fig. 4). Let divergent laser light enter the interferometer and consider equation (5) setting  $\alpha_R$  equal to zero. If  $a$  is constant over the field of view, then the phase  $\phi/2$  is constant on curves  $\varphi = \text{const}$ . Curves where  $\phi/2$  is a multiple of  $\pi$  are bright, these are the Haidinger fringes. To generate them over the whole field of view put a lens of short focal distance in front of the beam expander to illuminate the interferometer plates over their complete area. Place a diffuser plate immediately under the interferometer, put mirror  $M_2$  away and look from above into the instrument with one eye, accommodated at infinity. Check if the diameter of an individual ring in the concentric fringe system is constant when your eye is over those points where the plates lie on

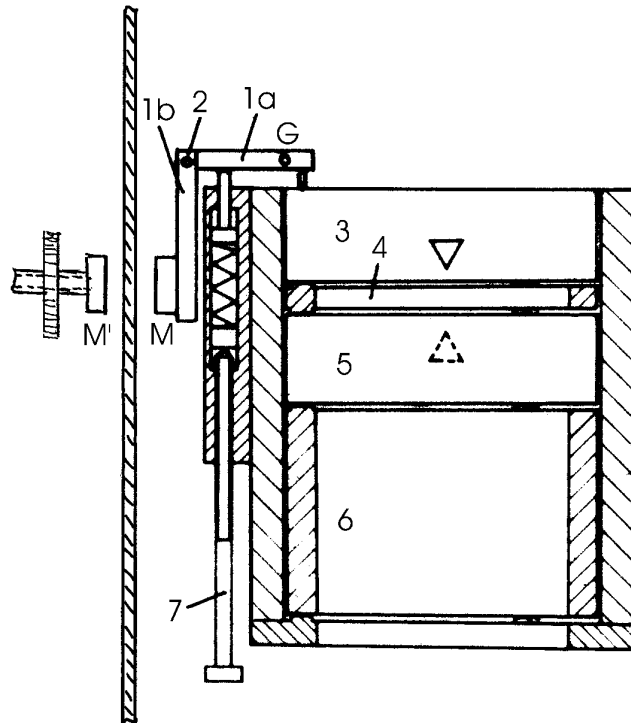


Figure 10: The mount of the interferometer plates and the mechanics of their fine adjustment

the etalon ring. Think what it means if the circular fringes shrink or grow when you move from one supporting point to another. Remember that  $\phi/2$  remains constant on an individual fringe independent of its diameter. Approaching or removing the magnets  $M'$  you can achieve that the plates are parallel.

**As a precaution the magnets  $M'$  must be as far away as possible from the wall of the interferometer recipient. This it to avoid unnecessary deformations or even damage of the plates.**

When the diameters of the Haidinger fringes keep constant at the three points of support you must still refine the adjustment procedure. Set the argon pressure in the interferometer so that in the center of the circular fringe system a new ring is just being created, that means a very faint reddish spot appears as the early stage of a Haidinger ring. You can watch the birth of a ring from your position where you handle the needle valve; just put mirror  $M_2$  back on the interferometer but rotated horizontally by  $120^\circ$  and stop the gas flow at the right moment. Adjust the magnets  $M'$  so that the very faint spot has the same brightness at the three points at the plate suspension. However, as the flatness of optical elements is not guaranteed up to their edges, you should position your eye such that the reddish spot is a bit away from the edge of the plates. And yet the distances

should be the same at all three checkpoints, because the brightness of the laser beam increases radially towards its axis. Use the smallest Haidinger ring to keep a constant gap to the border of the plates (Fig. 11).

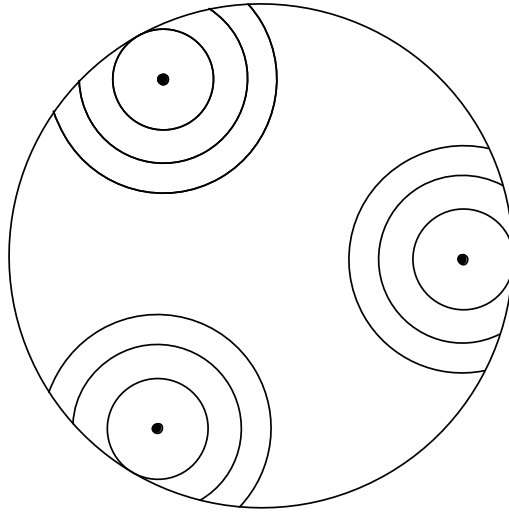


Figure 11: Position of Haidinger rings at the three points of support

## 6 Setting the Instruments

### 6.1 The monochromator

The monochromator acts as a wavelength filter, as a spatial filter, and as a diaphragm decreasing the brightness on the cathode of the attached photomultiplier. Set the gratings at the angle for laser light (632.8 nm) indicated on the body. Open the entrance slit until the tangential image of the laser spot (a vertical line) just disappears between the slit jaws and limit the slit length just like that; there is a pair of jaws on the slit body to act on the length. Thus the aberrated images are kept away. The true image should not be intersected by the slit jaws because it could introduce a jitter of the photomultiplier signal. Although to total mount (table, optical bench, etc.) is rather stiff, vibrations may happen leading to a deflective oscillation of the laser image relative to the slit jaws. The intermediate and the exit slit of the monochromator must be set so that the image of the entrance slit is fully transmitted. As the magnification of the spectrometer is unity you may set the three slits at the same width although this is not the optimum setting.

When the slits are so large the photomultiplier can get too much light. To protect it from damage close the diaphragm on lens  $L_2$  as far as possible. You can open it under control when the photomultiplier and the recorder are switched on.

## 6.2 The recorder

Apart from plotting the hyperfine structure spectrum and the Airy function the recorder serves as current meter of the photomultiplier current while optimal settings of all optical elements are being found. The indication of the recorder pin is proportional to the voltage signal at the input and the input impedance is  $1\text{ M}\Omega$  at all ranges down to  $50\text{ mV}$ . Sensitivity ranges below this figure cannot (and need not) be applied without an interface transforming the anode current of the photomultiplier into a voltage signal on a low impedance ( $I/U$  amplifier). As the signal generated at the recorder input has opposite sign with respect to the voltage between the last stage and the anode of the photomultiplier the sensitivity range of the recorder should be a few volts at most to avoid nonlinear feedback. As far the paper transport, set the speed at  $20\text{ mm/min}$  to plot the Airy function and at  $1\text{ mm/min}$  when you check the stability of the overall mount.

## 6.3 The photomultiplier

At last the power supply for the photomultiplier is switched on. Select  $550\text{ V}$  for the measurements with laser light and  $850\text{ V}$  for the hyperfine structure of the mercury lines. When you switch on the voltage, you can see from the little swing of the recorder pin, if the electrical circuitry is alright. To check whether the junction between the photomultiplier and the exit slit is tight, increase the sensitivity range of the recorder and switch off the light. There must be no change of the recorder indication.

## 6.4 Optimizing the signal and test measurement

Let argon enter extremely slowly and watch the recorder pin (no paper transport). At about  $150\text{ mbar}$  there is the first maximum of the Airy function, when laser light is applied. Stop the gas flow at this pressure, bring the recorder signal at maximum by refining the settings of the wavelength at the monochromator, of the pinhole in the pinhole disk, and of the inclination of mirror  $M_2$ . By means of the diaphragm on lens  $L_2$  and of the variable switch on the recorder panel you can stop the recorder signal at a sufficient height on the scale on the paper. The Airy function is extremely narrow, the finesse being about 30. If you have failed the first maximum for this tuning, wait for the next one and stop the gas there.

Make a test run until one or two maxima of the Airy function have passed to see if everything is as you like it to be. The gas flow must have a rate of about  $5\text{ mbar/3sec}$ . Check in the test run if the maximum of the Airy function gets to the same height as before at constant pressure. When the gas streams too fast into the interferometer, the recorder cannot follow and the Airy curve will be integrated. The time constant of the recorder is about one second. When the test run was successful fill liquid nitrogen into the trap, if you have not done it before, and pump off the argon. Now the measurements can begin.

## 7 Measurements with the He–Ne Laser

### 7.1 Measuring the Airy function

Make some full runs from  $p \approx 0$  to atmospheric pressure, each at a different diameter of the diaphragm on  $L_2$ . When you have doubts if the interferometer plates are aligned at best, check it again.

### 7.2 Stability of the total experiment

You will remark that within the same run the maxima of the Airy function are not constant. To find the reason stop the gas stream as close as possible at one of these maxima and plot the photomultiplier signal at constant pressure with 1 mm/min paper transport. Wait until you have a plot of about 20 mm and interpret the signal.

## 8 Measurements of the Hyperfine Structure of Mercury Lines

### 8.1 Change of the optical mount

The laser and its beam expander must be replaced by the mercury lamp and the objective  $L'_1$ , Fig. 12.

#### a) Adjustment of the objective $L'_1$

At first when the laser is still switched on put  $L'_1$  over the large hole in the table carrying the interferometer body. By means of the laser ray (put the cap on the beam expander) you can easily find the position of  $L'_1$  at which the laser ray is centered on the pinhole disk and on the entrance slit as before without  $L'_1$ . Now you must not touch  $L'_1$  anymore.

#### b) Adjustment of the mercury lamp

Slide the deflecting mirror  $M_1$  away and replace it by the mercury lamp. Put the little piece of cardboard with the slit on the lamp so that the slit is centered on the discharge tube and touches it. Unless the slit is too far away from the optical axis of  $L'_1$ , you can see now the image of the slit on the cardboard in autocollimation. Adjust the lamp so that the slit and its image coincide and the image is sharp on the cardboard. When this adjustment is finished remove the cardboard. A bright image of the Hg lamp is now visible on the pinhole disk interspersed with beautiful centered Haidinger rings. The central spot of this fringe system must precisely hit the pinhole and the entrance slit. If not, correct the alignment of the lamp. Anyway, finally refine the alignment while observing the recorder signal as described already. Of course, you must have changed the wavelength at the monochromator before.

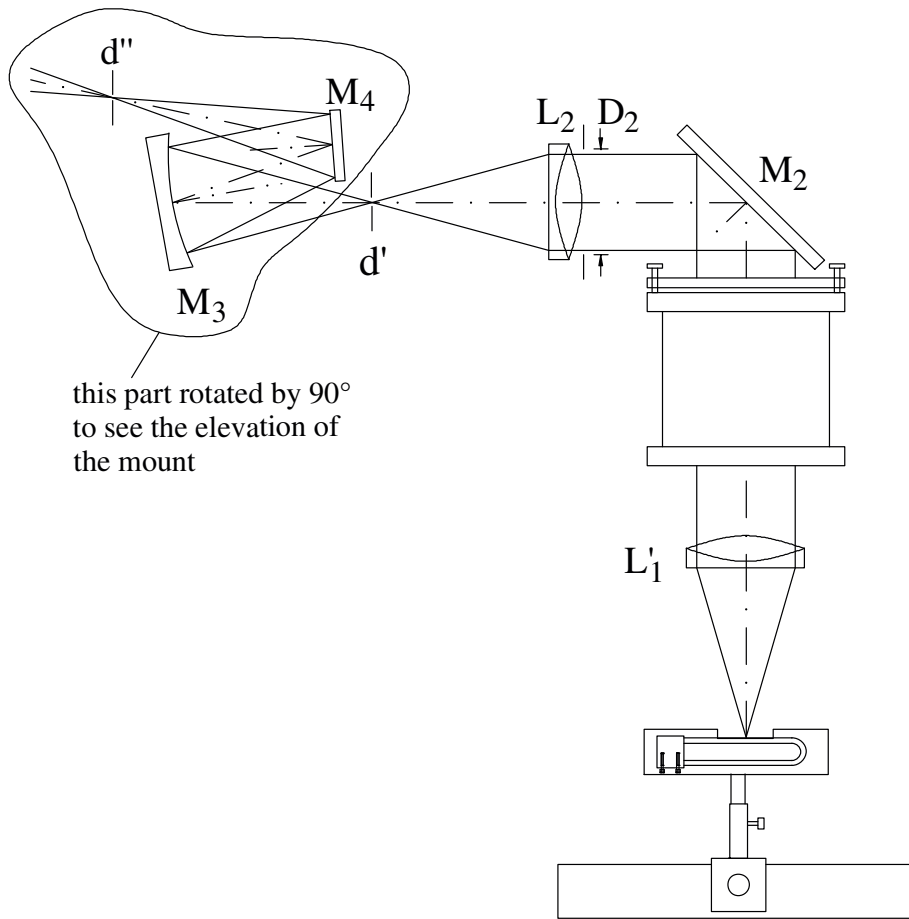


Figure 12: Aligning the mercury lamp

### c) Control of the adjustment of the interferometer plates

Once precisely adjusted the parallelism of the plates is very stable. However, the action of the levers on the plates (Fig. 10) is mechanical, so there is friction and consequently hysteresis in finding the correct position. Apart from this effect, there are aberrative beams (Sect. 5.5 d) generating fringes, too, which makes the adjustment difficult with laser light. The adjustment thus achieved can be controlled with the mercury lamp mounted now. The procedure is the same as described in Sect. 5.6. Slide the diffuser plate directly under the body of the interferometer and expand the beam of mercury light by putting a divergent lens on the objective  $L'_1$ . Handle carefully in order not to displace  $L'_1$ . Stop the gas flow when you see a green spot (green Hg line at 546 nm) of sufficient brightness in the center of the fringe system. Like with laser light, check the brightness of the spot at the positions of the three magnets. Correct eventually.

## 8.2 Measurements with the mercury lamp

### a) Tolerable beam divergence and area of the plates for best resolution

Make a run of measurements plotting the photomultiplier signal only for one or two periods (interference orders) of spectrum of the green Hg line at 546.07 nm. Keep the slit widths constant at 1 mm and change each time the size of the pinhole  $d'$  up to 1 mm, the slit width. Look for the best spectral resolution. To compare the results it is recommended to tune the maxima in the plots at equal height by means of the variable switch on the recorder panel. The diameter of the pinhole has an impact on the total finesse  $F$  in (17), Sect. 3, because it defines the divergence of the beam generating the interference pattern.

Try also to improve the spectral resolution by decreasing the free area of the interferometer plates, i.e., reduce the diaphragm  $D_2$  on  $L_2$ . You can combine the reduction of  $D_2$  with the dilation of  $d'$ . Depending on the precision of your alignment and also on the partition of flatness over the area of the interferometer plates, a reduction of  $D_2$  can improve the corresponding part of the finesse, see again (17). Therefore, the still tolerable size of the pinhole may depend upon the diameter  $D_2$  and the combination of both changements makes sense.

### b) Measuring the hyperfine structure of mercury lines

Make at least one full run from  $p \approx 0$  to atmospheric pressure for the green line at 546.07 nm and the violet one at 404.6 nm. Check if the maxima are strictly equidistant and reveal the atmospheric pressure.

## 9 Evaluation and Analysis

### 9.1 The finesse

Determine the finesse from your measurements with the laser for different diaphragms on  $L_2$ . Is the finesse as could be expected from (15), Sect. 3.2? Comment the result! The following list with the parameters of the instrument might be useful:

|   |                              |
|---|------------------------------|
| wavelength of He–Ne laser                           | $\lambda = 632.8 \text{ nm}$ |
| reflection coefficient of the interferometer plates | $R = 0.94$                   |
| gap between the plates                              | $a = 5.231 \text{ mm}$       |
| flatness of the plates                              | $\lambda/50$                 |
| pinhole in the beam expander                        | $30 \mu\text{m}$             |
| expansion ratio                                     | 25                           |
| focal distance of objective $L_1$                   | $\approx 15 \text{ cm}$      |
| focal distance of objective $L'_1$                  | 30 cm                        |
| focal distance of $L_2$                             | 30 cm                        |
| focal distance of mirror $M_3$                      | 15 cm                        |

Check if the peaks in the Airy function are rigorously equidistant and comment an eventual deviation.

## 9.2 The stability

List the possible causes to explain the photomultiplier signal plotted in Sect. 7.2. Then note all causes that must be excluded and tell why. You will arrive at the conclusion that the laser itself must be the source of instability. There are two possibilities to expose such a behaviour, i.e., the intensity and the frequency of the laser light. Analyse and comment!

## 9.3 The refractive index of argon

From the plot with laser light and from that one with the mercury lamp you can easily determine the refractive index of argon. First make clear that  $n - 1$  is proportional to the pressure of argon inside the interferometer. In nearly all textbooks on optics there is a chapter on dispersive media, theory of dispersion, propagation of light in matter, or something like that. There you find for low density media with  $n \approx 1$  the dispersion formula  $n(\omega)$ , i.e.,

$$n^2 = (n + 1) \cdot (n - 1) \approx 2(n - 1) = \omega_p^2 \sum_j \frac{f_j}{\omega_j^2 - \omega^2 + i\gamma_j\omega} \quad (22)$$
$$\text{with } \omega_p^2 = \frac{N^2 e}{m\varepsilon_0}$$

with the following meanings:

- $\omega_p$  plasma frequency of the gas,
- $N$  density of particles, where  $N \sim p$  because of  $p = NkT$ ,
- $e, m$  charge and mass of an electron,
- $\varepsilon_0$  dielectric constant of vacuum,
- $\omega$  frequency of the light wave,
- $\omega_j, \gamma_j$  resonance frequencies and corresponding damping constants of the gas,
- $f_j$  oscillator strengths corresponding to the resonant frequencies,  $f_j$  is that part of the  $N$  particles which oscillates at the resonance frequency  $\omega_j$ .

In every maximum of the Airy function the optical path  $na$  is a multiple of  $\lambda/2$ . Establish this relation for  $p \approx 0$  and for atmospheric pressure and subtract one from the other to get the refractive index  $n$  of argon. For comparison one can take  $n$  from D'Ans-Lax, Physikalische Tabellen, it is

$$n = 1.00028 \quad \text{at} \quad 760 \text{ Torr} .$$

## 9.4 Analysis of the hyperfine structure spectra

According to (6), Sect. 2, the maxima of the Airy function are characterized by

$$2na\sigma \cos \varphi = m , \quad (23)$$

where  $m$  is an integer called order of interference. Let  $m_1$  be the order of interference of the first maximum after  $p = 0$  and may  $z$  design the current number of maximum starting with  $z = 1$ , which is the first maximum after  $p = 0$ . Then it can be written instead of (23)

$$2na\sigma \cos \varphi = m_1 + z - 1 , \quad (24)$$

which at  $p = 0$  (i.e.,  $n = 1$ ) becomes

$$2a\sigma \cos \varphi = m_1 - \varepsilon , \quad \text{with } 0 < \varepsilon < 1 . \quad (25)$$

The corrective  $\varepsilon$  at the interference order  $m_1$  in (25) is necessary because the term on the left side is generally a fractional number instead of integer.

One of the goals of the experiment is to determine  $\sigma$  for the individual components of hyperfine structure. It may seem obvious to plot  $n$  over  $z$  in (24) and to find  $\sigma$  for every line of the hyperfine structure from the slope of the corresponding curve (straight line), but the idea cannot be realized. The slope must be measured with a precision of  $10^{-5}$ , which is impossible. Therefore another way must be found.

As mentioned it is

$$n - 1 = Kp , \quad (26)$$

the coefficient  $K$  depending on  $\sigma$ . If we deduce (25) from (24) and respect (26), we obtain

$$p = \frac{1}{2Ka\sigma \cos \varphi} (z - [1 - \varepsilon]) , \quad (27)$$

which provides a straight line  $p(z)$  for every  $\sigma$  contained in the spectrum. The coefficient  $K$  is unknown, so again  $\sigma$  cannot be found from the slope. However,  $\varepsilon$  is easy to determine and the  $\varepsilon$  are clearly distinct for the individual straight lines. The method shall be explained in detail for the hyperfine structure of the green Hg line at 546.07 nm. The order of interference must get a second index, which will be  $o$  or  $i$ ;  $o$  designates the strong line the detailed structure of which is unresolved, whereas  $i$  stands for the individual component of hyperfine structure. The first index of  $m$  indicates the number of the maximum since  $p = 0$ , as before. According to (25) there are at  $p = 0$  the relations for the strong line and the hyperfine structure component  $i$ ,

$$\begin{aligned} 2a\sigma_i \cos \varphi &= m_{1i} - \varepsilon_i , \\ 2a\sigma_o \cos \varphi &= m_{1o} - \varepsilon_o , \end{aligned}$$

where the meaning of  $\varepsilon_i$  and  $\varepsilon_o$  is like in (25). Subtracting the second equation from the first leads to the result

$$\Delta\sigma_i = \sigma_i - \sigma_o = \frac{m_{1i} - m_{1o} - \varepsilon_i + \varepsilon_o}{2a \cos \varphi}$$

or, when  $\Delta\sigma$  will be replaced by  $-\frac{\Delta\lambda}{\lambda^2}$ ,

$$\Delta\lambda_i = \lambda_i - \lambda_o = -\frac{\bar{\lambda}^2}{2a \cos \varphi} \left[ \underbrace{m_{1i} - m_{1o}}_{\Delta m_i} - \underbrace{(\varepsilon_i - \varepsilon_o)}_{\Delta \varepsilon_i} \right], \quad (28)$$

$\bar{\lambda}$  is the mean of  $\lambda_o$  and  $\lambda_i$ ; it is  $\bar{\lambda} \approx \lambda_o$ . With a good alignment  $\varphi$  can be set equal to zero,  $a$  is a given parameter of the interferometer (here  $a = 5.231$  mm), so the individual  $\Delta\lambda_i$  or  $\Delta\sigma_i$  respectively can be obtained with (28). Draw a straight line for each component  $\lambda_i$  directly on the plot taken from the recorder (Fig. 13). The calibration of the pressure plotted on the time axis is not needed, it must only be guaranteed that  $p$  is proportional to  $t$ . The values of the  $\Delta\varepsilon_i$  can unambiguously be revealed from the constructed straight lines, whereas  $\Delta m_{1i}$  cannot be found. To see the problem, calculate the free spectral range from (9), Sect. 3.1, and compare with the spectrum in the following table, which can be found in [3] and [6],

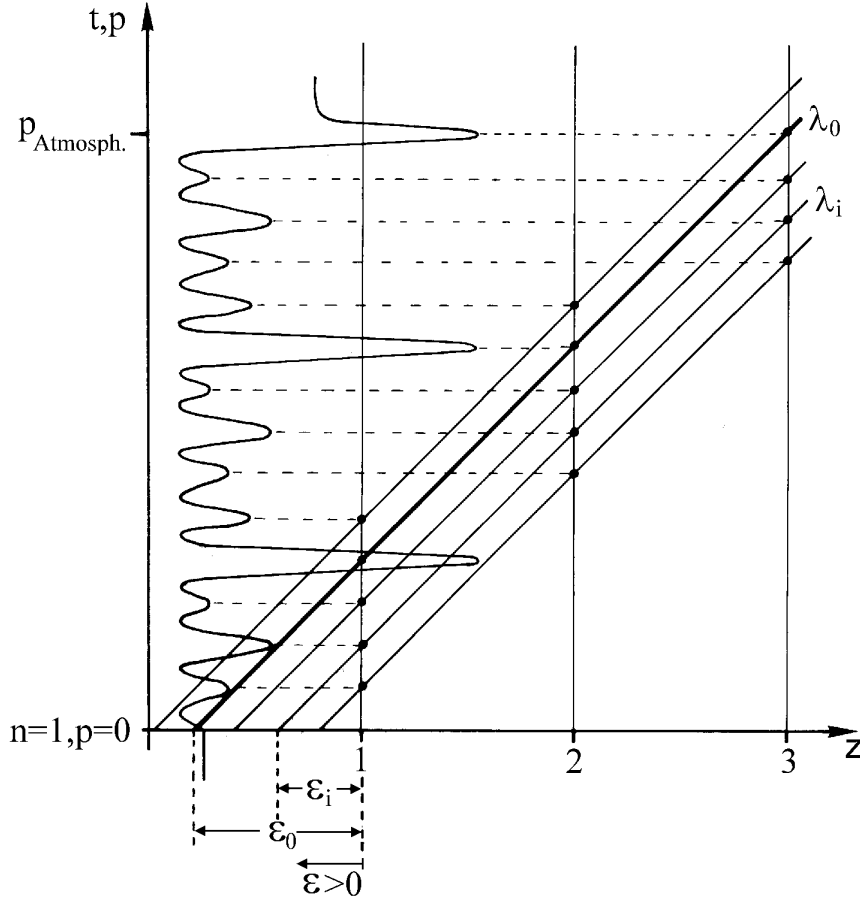


Figure 13: The recorder plot with the hyperfine structure and the straight lines for their evaluation

|                            |       |       |      |      |       |       |       |       |
|----------------------------|-------|-------|------|------|-------|-------|-------|-------|
| $\Delta\lambda_{i/pm} [ ]$ | +21.4 | +12.8 | +8.5 | -6.9 | -10.2 | -23.6 |       |       |
| $\Delta\lambda_{i/pm} [ ]$ | +20.8 | +12.2 | +7.8 | -2.7 | -5.5  | -7.6  | -10.9 | -24.3 |

You will come to the result that there must be an overlap of different interference orders. So the interference order  $m_i$  of line number  $i$  has an uncertainty of 1. However, the uncertainty is different, if  $\lambda_i > \lambda_o$  or  $\lambda_i < \lambda_o$  and if line number  $i$  comes before or after line number  $o$  to a maximum when counting from  $p = 0$ .

Get the  $\Delta\varepsilon_i$  from the construction on the recorder plot and complete the table below.

| $\Delta m_i$                          | $\Delta\varepsilon_i$ | $\Delta m_i - \Delta\varepsilon_i$ | $\Delta\lambda_{i/pm}$ |
|---------------------------------------|-----------------------|------------------------------------|------------------------|
| $\lambda_i > \lambda_o, \Delta m_1 =$ |                       |                                    |                        |
| $\lambda_i < \lambda_o, \Delta m_1 =$ |                       |                                    |                        |
| $\lambda_i > \lambda_o, \Delta m_2 =$ |                       |                                    |                        |
| $\lambda_i < \lambda_o, \Delta m_2 =$ |                       |                                    |                        |
| $\vdots$                              |                       |                                    |                        |

To decide which of the two  $\Delta\lambda_i$  found for every  $\Delta\varepsilon_i$  is correct, compare with the table above. Determine the finesse again, this time from the plot of the mercury line just analysed. Your result will be much worse than that obtained with the laser (about 7 instead of 25...30 there). Comment!

A hint: For the interferometer the laser line is a  $\delta$  function in spite of the very high spectral resolution. What about the mercury line? Estimate the halfwidth of its emission due to the Doppler effect. This is a good occasion to look into your course on thermodynamics and statistics (Physik IV).

## 10 Annex

### Interference by shearing of wavefronts and focalisation of lens $L_1$

Consider a beam of monochromatic light with little divergence entering a parallel flat of glass (Fig. 14). Apart from the transmitted light there are two beams reflected downward. They have nearly equal intensity and are laterally displaced with respect to each other. In the common part of their section interference fringes can be observed. The phase difference between the wavefronts is composed of delay and shear.

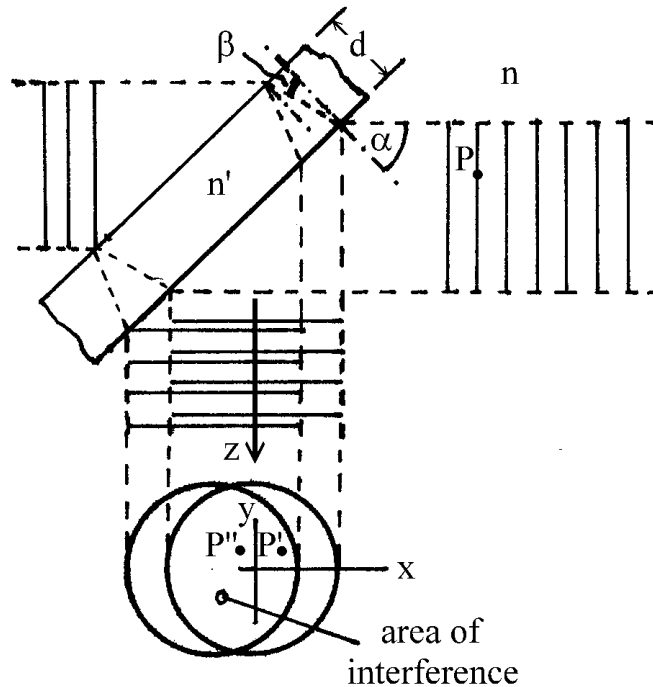


Figure 14: Delay and lateral shear of wavefronts

The delay. The beam from the backside of the flat has travelled a longer optical path than that one from the front. But without the mutual lateral shift of the beams there would be no interference pattern because the delay is the same for every pair of corresponding points  $P'$  and  $P''$  lying on one wavefront each. The common area would be homogeneously illuminated without any structure. However, if the little divergence (or convergence) supposed at the beginning of this section is not small enough or if the delay is sufficiently long, the points  $P'$  and  $P''$  will be radially displaced with respect to each other and, consequently, the wavefronts have a mutual radial deformation. Under these conditions a pattern will arise again. If there is a pure delay and no lateral dislocation or radial deformation of the two beams, there is no pattern. The brightness on a screen

then ranges somewhere between totally dark and fully bright depending on the optical path difference, that means  $d$ ,  $n'$ , and  $\alpha$ .

The shear. The lateral displacement of wavefronts with respect to each other is called lateral shear. Unless the wavefronts are plane, shearing introduces a phase shift between two points which belong to different wavefronts but have the same coordinates. Let  $W(x, y)$  be the deviation of the phase from that of a plane wave in the  $x, y$  plane.

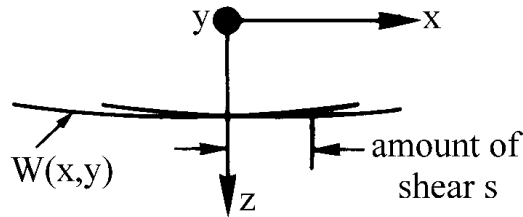


Figure 15: Shear of two wavefronts

If the refractive index  $n$  is constant then  $W(x, y)$  is the geometrical form of the wavefront. Anyway, when  $\vec{s}$  is the shear which one of the beams has undergone with respect to the other, then  $\vec{s} \text{ grad } W(x, y)$  is the phase difference between the two wavefronts at point  $x, y$ . In Fig. 15 the shearing vector  $\vec{s}$  is parallel to the  $x$  axis, so the curves of equal phase difference are

$$\vec{s} \text{ grad } W(x, y) = s \frac{\partial W(x, y)}{\partial x} = m\lambda . \quad (29)$$

These curves are the fringes in the interference pattern. The fringes are

bright, where  $m$  is an integer,  
 dark, where  $m$  is an odd multiple of  $\frac{1}{2}$ .

Rigorously Eq. (29) holds only for an infinitesimal shearing  $\vec{s}$ . The function  $W(x, y)$  may describe any kind of wavefront deformation, including aberrations and defocussing. From the shape of the shearing fringes in (29),  $\text{grad } W(x, y)$  can be obtained and  $W(x, y)$  revealed. In shear interference a wavefront is compared with itself after an (infinitesimal) lateral displacement, no reference wavefront is needed. It is a simple and powerful method to check wavefronts for deformations.

Focussing lens  $L_1$ . If the pinhole in the beam expander (Fig. 7) is outside the focal plane of  $L_1$ , the beam which enters the interferometer is convergent or divergent. By means of a shearing plate like that in Fig. 14 a pattern of lateral shearing fringes can be generated. It indicates the change of convex to concave wavefronts when the pinhole is positioned in the focal plane.

When  $W(x, y)$  consists of defocussing only, one gets from Fig. 16

$$z = W(x, y) = R(1 - \cos \varphi)$$

with

$$\sin \varphi = \frac{r}{R} = \frac{\sqrt{x^2 + y^2}}{R}$$

and therefore

$$W(x, y) = R \left( 1 - \sqrt{1 - \frac{x^2 + y^2}{R^2}} \right).$$

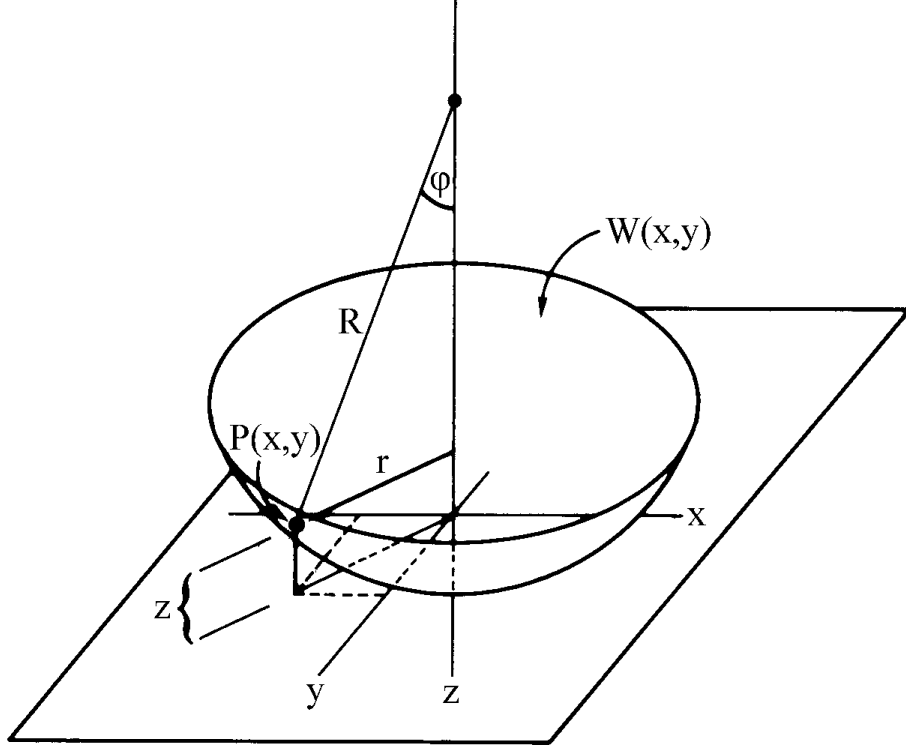


Figure 16: The spherical wavefront  $W(x, y)$

For the paraxial or Gauss' approximation,  $x^2 + y^2 \ll R^2$ , it is

$$W(x, y) = R \left( \frac{1}{2} \frac{x^2 + y^2}{R^2} + \frac{1}{8} \left[ \frac{x^2 + y^2}{R^2} \right]^2 + \dots \right) \approx \frac{x^2 + y^2}{2R}. \quad (30)$$

Let the shear vector  $\vec{s}$  have the direction of the  $x$  axis, then the equation of the fringes is, according to (29),

$$\frac{s}{R} x = m\lambda. \quad (31)$$

So the fringes are straight lines parallel to the  $y$  axis and at right angles to the direction of shear. The spacing between two fringes is

$$\Delta x = \frac{\lambda R}{s}, \quad (32)$$

infinite spacing indicates parallel light. But when the gap between neighbour fringes exceeds the field of view the control over  $R$  is lost. However, when you slightly press against the frame of the shearing plate in order to deform the mechanical mount, you can make the neighbour fringes re-enter the field of view, although not simultaneously. But you have nevertheless an estimation whether the fringe spacing increases or decreases by your further manipulations with the pinhole position relative to  $L_1$ .

The shear  $s$  can easily be calculated from Fig. 14. It is

$$s = \frac{nd \sin 2\alpha}{\sqrt{n'^2 - n^2 \sin^2 \alpha}} . \quad (33)$$

Inserting  $s$  in (31) and (32), one obtains for positioning and spacing of the fringes

$$\frac{nd \sin 2\alpha}{R\sqrt{n'^2 - n^2 \sin^2 \alpha}} x = m\lambda , \quad (34)$$

$$\Delta x = \frac{\lambda R\sqrt{n'^2 - n^2 \sin^2 \alpha}}{nd \sin 2\alpha} . \quad (35)$$